Influence of thermocycling on the functional properties of the NiTi alloy produced by wire arc additive manufacturing

NOTE

Influence of thermocycling on the functional properties of the NiTi alloy produced by wire arc additive manufacturing

Engineering Research Express

CrossMark

RECEIVED
14 November 2023

REVISED
5 May 2024

ACCEPTED FOR PUBLICATION
16 May 2024

PUBLISHED
28 May 2024

NOTE

Influence of thermocycling on the functional properties of the NiTi alloy produced by wire arc additive manufacturing

Rashid Bikbaev[1], **Natalia Resnina**[1], **Palani Anand Iyamperumal**[2], **Sergey Belyaev**[1] and **Geethapriyan Thangamani**[2]

[1] Saint-Petersburg State University, 7/9 Universitetskaya nab., Saint-Petersburg, 199034, Russia
[2] Department of Mechanical Engineering, Indian Institute of Technology Indore, Indore 453552, India

E-mail: BikbaevRM@yandex.ru

Keywords: Shape memory alloys, WAAM, thermal cycling, recoverable strain variation

Abstract

The influence of the thermocycling under a stress of 200 and 300 MPa on the martensitic transformation temperatures, recoverable and irreversible strain was study in the NiTi samples produced by wire arc additive manufacturing (WAAM). Two types of samples were used: the T1 sample including the Ti-rich NiTi and Ni-rich NiTi layers in the working length and the T2 sample including only the Ni-rich NiTi layers. It was found that the variation in the martensitic transformation temperatures on thermal cycling depended on the chemical composition of the layer. The transformation temperatures decreased on thermal cycling in the Ti-rich NiTi layer (in T1 sample), whereas they were constant in the Ni-rich NiTi layers (in T1 and T2 samples). The recoverable strain in both samples did not change during thermal cycling. The irreversible strain was found in the T1 sample regardless of stress acting on thermal cycling, while T2 sample showed the plastic strain only in the first cycle under 300 MPa. It was shown that the difference in a functional behavior of the T1 and T2 samples on thermocycling was due to that the T1 sample contained the Ti-rich NiTi layer, that was characterized by a low dislocation slip limit contrary to the Ni-rich layers which were hardened by the Ni_4Ti_3 precipitates.

1. Introduction

Shape memory alloys are functional materials showing a unique ability to recover unelastic strain on heating (shape memory effect) or unloading (superelasticity) that make them to be promising for applications in space, medicine, and robotics [1–3]. Among the shape memory alloys, the NiTi alloys demonstrate large shape memory effect, superelasticity and good mechanical properties so these alloys are promising for application [2, 3]. However, the poor workability of NiTi-based alloys limits their extensive utilization as products with complex shapes. This problem may be solved by using the additive manufacturing: by selective laser melting (SLM) or wire-arc additive manufacturing (WAAM). The SLM was comprehensively studied earlier and this technique is more suitable for production of small size objects [4]. The WAAM is more preferable for the production of large size objects due to a high rate for the manufacturing. The properties of the NiTi samples produced by WAAM have been studying since 2019 and main results are published in [5–23].

Previously it was shown that the NiTi samples produced by WAAM demonstrated all shape memory effects [6–11, 13–18, 23]. However, their structure and martensitic transformations differed significantly from the NiTi alloys produced by conventional techniques [5, 7, 10, 13]. The main feature was that the chemical composition of the NiTi phase in various layers was different [9–11] that significantly affectd the martensitic transformation temperatures [1]. Moreover, the different layers were characterized by different volume fraction and the size of the precipitates [10] that additionally affected the transformation parameters [1]. Therefore, in the NiTi samples produced by WAAM, the martensitic transformations occurred at different temperatures in various layers [10]. The second feature was that the columnar grains formed due to the presence of the preferable direction for heat

transfer during solidification. As a result, [001] texture appeared that affected the functional properties [5, 7, 13, 15, 19, 20, 22] as it was observed in the NiTi alloys produced by conventional technique [24]. All these factors (chemical composition, texture, and the precipitates) affected the mechanical and functional properties of the NiTi samples produced by WAAM.

In many applications, the NiTi elements are subjected to repeating cooling and heating through a temperature range of the martensitic transformations. For such devices, a thermal cycling stability of the functional properties (martensitic transformation temperatures, recoverable strain) is the key factor. In the NiTi samples produced by conventional way, the thermal cycling stability of the properties depends on the chemical composition and the structure of the alloys which influenced the yield limit for dislocation slip [25–29]. In the equiatomic NiTi or quenched Ni-rich NiTi alloys, the dislocation yield limit was small, as a result, the plastic strain appeared during the formation of the martensite crystals that decreased the transformation temperatures in next cycles, affected the recoverable strain and increased the plastic irrecoverable strain [1, 25, 26]. At the same time, the annealed Ni-rich NiTi alloy was hardened by the Ni_4Ti_3 particles that increased the dislocation yield limit and prevented to an increase in defect density [1, 27]. As a result, the temperatures and recoverable strain remained constant while the irrecoverable plastic strain was small. Thus, the martensitic transformation temperatures as well as the recoverable and irrecoverable strain depend on the chemical composition of the NiTi phase and precipitates. As the NiTi samples produced by WAAM include the layers with different chemical composition of the NiTi phase and the precipitates distribution hence, the variation of the functional properties in various layers during thermal cycling may be different. As the NiTi samples produced by WAAM may be used for repeating action devices, hence the thermal cycling stability of the functional properties is the very important for application. The analysis of the published papers showed that the thermal cycling behaviour in the NiTi samples produced by WAAM had never been studied. Therefore, the aim of the paper was to study the stability of martensitic transformations and strain variation during thermocycling under constant stress in the NiTi samples produced by WAAM.

2. Materials and methods

Five-layered NiTi sample was deposited on Ti substrate (a thickness of 8 mm) by wire arc additive manufacturing, using the $Ni_{50.9}Ti_{49.1}$ wire with a diameter of 1.2 mm as feedstock (the details of the deposition parameters were presented in [10]). The cross-section plates with a thickness of 0.5 mm were cut from as-built sample by Electrical Discharge Machine 'Arta 153 Pro'. These plates were used to cut the dog-bone samples for tensile test with a working length of 6 or 10 mm, a width of 1 mm and a thickness of 0.5 mm (figure 1(a)-b). Previously in [10], it was shown that the variation in chemical composition and precipitate distribution was observed in first four layers. So, to obtain the samples with various structure of the layers, it is necessary to include these layers in the working length subjecting to deformation. Thus, two types of samples were used: the T1 sample included the 2nd—4th layers and the T2 sample included the 3rd—4th layers in the working length as shown in figure 1. The samples were subjected to annealing at 450 °C for 10 h (these parameters were chosen on the basis of the results [9, 12, 18]). After such heat treatment, the 2nd layer contained the Ti–rich NiTi phase and coarse Ti_2Ni precipitates on the grain boundaries which formed during manufacturing. The 3rd layer included the Ni-rich NiTi phase with fine Ti_2Ni precipitates on the grain boundaries which formed during manufacturing. The 4th layer had the Ni-rich NiTi phase with fine Ni_4Ti_3 precipitates formed during annealing (figure 1(c)). Thus, the T1 sample included the 2nd layer with Ti-rich NiTi phase and Ti_2Ni precipitates; the 3rd and 4th layers with the Ni-rich NiTi phase and Ti_2Ni or Ni_4Ti_3 precipitates. The T2 sample had the 3rd and 4th layers with the Ni-rich NiTi phase and Ti_2Ni or Ni_4Ti_3 precipitates.

To study the martensitic transformation, small samples were cut from the 2nd, 3rd and 4th layers of the annealed samples. The martensitic transformations were studied by differential scanning calorimetry (DSC) in a Mettler Toledo 822e apparatus on cooling and heating at a temperature range of 140 °C to −110 °C (cooling/heating rate was 10 °C/ min) (figure 2).

The martensitic transformation temperatures were determined according to ASTM standard and presented in table 1. It is seen that even after annealing at 450 °C for 10 h, the transformation temperatures and sequences were different in various layers. The 2nd and 3rd layers underwent the B2 ↔ B19′ transformation, whereas the 4th layer demonstrated the B2 → R → B19′ transformations on cooling and the B19′ → B2 transformation on heating. The formation of the R phase on cooling was due to the presence of the Ni_4Ti_3 precipitates in the NiTi matrix (figure 1(c)) [1].

'Lloyd 30k Plus' testing machine equipped with a thermal chamber was used to study the influence of thermocycling on functional properties of the NiTi alloy produced by WAAM. The special inter-grippers were used to fix the sample in the standard grips of the testing machine (see details in [10]). The stress was measured as the ratio of force detected by a standard S-shaped force cell to cross-section square. The strain was measured by

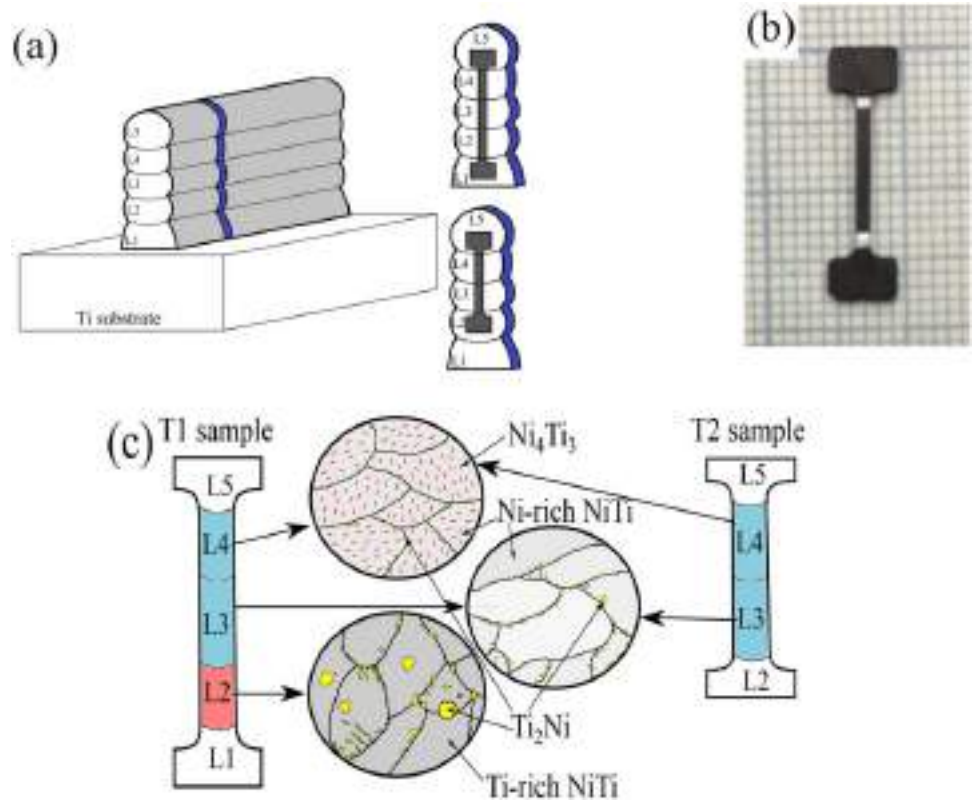

Figure 1. The scheme of the cutting of the T1 and T2 samples for tensile test (a). L1-L5 numbers of the layers from the bottom to the top of the sample. Image of the T1 sample (b). The scale paper has step of 1 mm. The scheme of the structure in the layers of T1 and T2 sample (c).

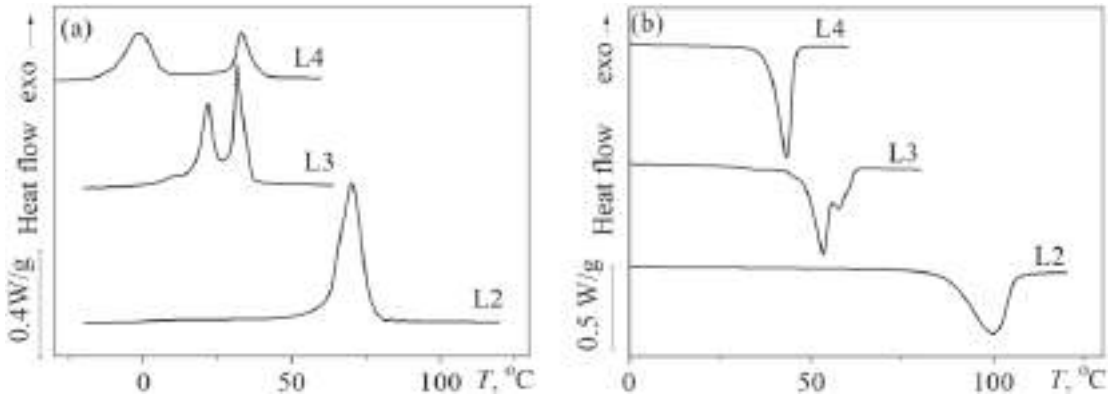

Figure 2. Calorimetric curves obtained on cooling (a) and heating (b) of the samples cut from 2–4 layers of annealed 5-layered NiTi sample. L2–L4—layer's number.

video extensometer as the variation in the gap between two white marks on the sample surface. The working length between two marks included the 2nd – 4th layers in the T1 sample, and the 3rd – 4th layers in the T2 sample. The sample was heated to a temperature at which all layers were in the austenitic state, loaded by 200 or 300 MPa and subjected to 10 thermocycles through the temperature range of the martensitic transformation under constant stress.

3. Results and discussion

Figure 3 showed the strain variation on the first cooling and heating of the T1 and T2 samples under a stress of 200 or 300 MPa. It is seen that the strain variation in the T1 sample occurred in some stages regardless of stress (figures 3(a), (c). The first stage on cooling starts at temperature of 73 °C and finishes at a temperature of 55 °C

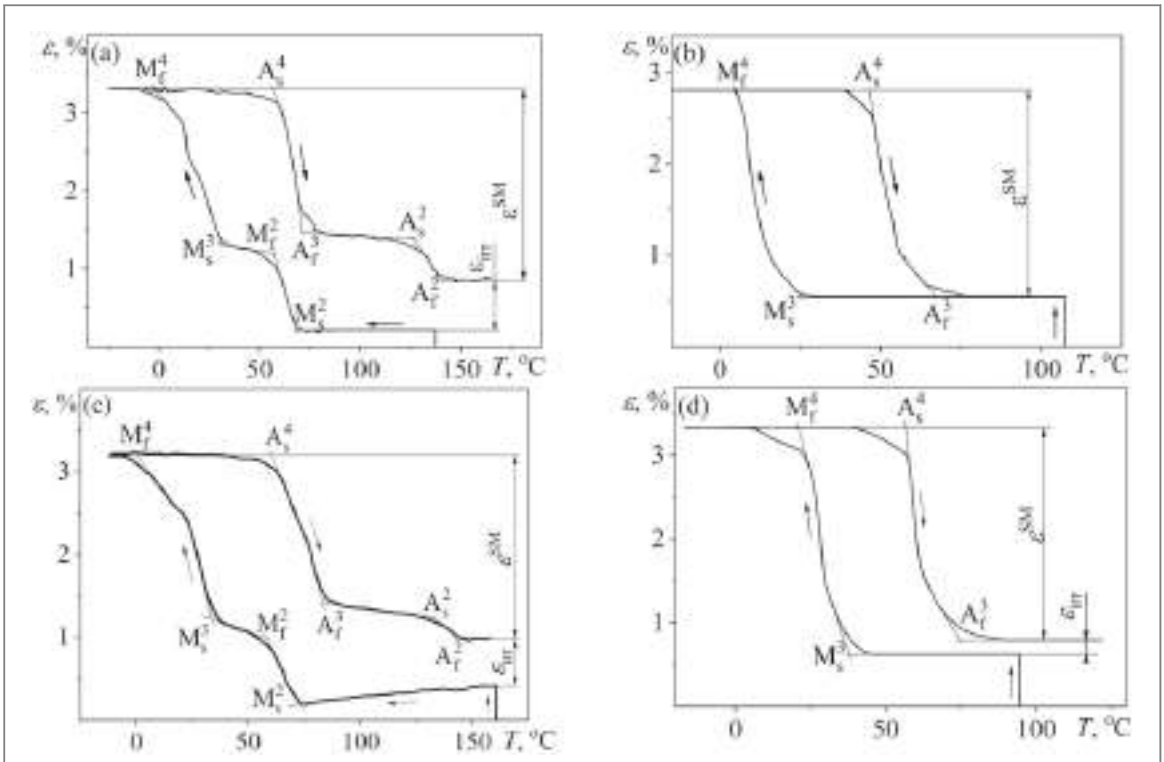

Figure 3. The dependences of the strain (ε) on the temperature (T) on the first cooling and heating of the T1 (a), (c) and T2 (b), (d) samples under a stress of 200 MPa (a), (b) or 300 MPa (c), (d). The layer number was indicated as upper case of the martensitic transformation temperatures.

Table 1. Structure and parameters of martensitic transformations in different layers of the NiTi sample produced by WAAM and annealed at a 450 °C for 10 h. The start (M_s) and finish (M_f) temperature of the forward martensitic transformation, the start (A_s) and finish (A_f) temperature of the reverse martensitic transition. The layer number was indicated as upper case of the martensitic transformation temperatures. The B2 is the austenite phase, the B19′ is the monoclinic martensite structure and the R is rhombohedral martensite phase.

Layer	Structure	Cooling		Heating	
		Transformation		Transformation	
2	$Ti_{50}Ni_{50} + Ti_2Ni$	B2 → B19’	M_s^2 =79 °C;	B19’ → B2	A_s^2 =85 °C;
			M_f^2 =61 °C		A_f^2 =106 °C
3	$Ti_{49,6}Ni_{50,4} + Ti_2Ni$		M_s^3 =37 °C;		A_s^3 =47 °C;
			M_f^3 =16 °C		A_f^3 =62 °C;
4	$Ti_{49,4}Ni_{50,6} + Ti_3Ni_4 + Ti_2Ni$	B2 → R	R_s^4 =41 °C;		A_s^4 =36 °C;
			R_f^4 =29 °C		
		R → B19	M_s^4 =8 °C;		A_f^4 =46
			M_f^4 = −14 °C		

whereas, the second stage of the strain variation starts at 27 °C and finishes below zero. The comparison of these temperatures to the transformation temperatures given in table 1 and in figure 2(a) showed that the first stage on the ε(T) curve was within the temperature range of the B2 → B19’ transformation in the 2nd layer (the temperatures of this stage were denoted as M_s^2 and M_f^2). The second stage of the strain variation on cooling was within the temperature range of the B2 → B19’ transformation that occurred in the third and fourth layers (see table 1, figure 2(a)). As the M_s temperature of the B2 → B19’ transformation in the 3rd layer was larger than in the 4th layer, hence it was clear that the transformation started in the 3rd layer. The M_f temperature in the 4th layer was less than in the 3rd layer, hence the strain variation finished in the 4th layer. Thus, the temperatures of the second stage of the strain variation on cooling was denoted as M_s^3 and M_f^4.

The strain recovery on heating of the T1 sample was also observed in two stages (figures 3(a), (c). The first stage was found within the temperature range of the reverse transformation in the 3rd and 4th layers; the temperatures of this stage was denoted as A_s^4 and A_f^3 (because the A_s temperatures in the 4th layer was the smallest, while the A_f temperature in the 3rd layer was the largest). The second stage of the strain recovery on

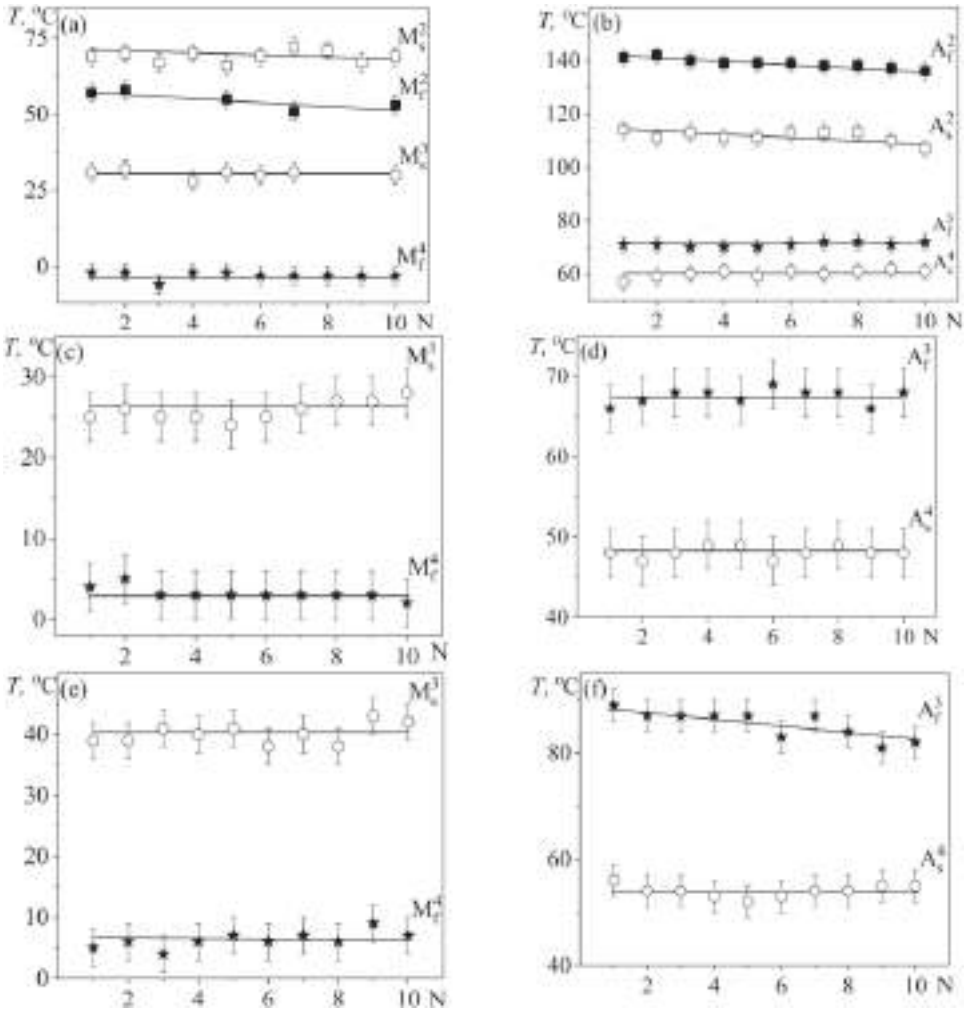

Figure 4. The variation in the temperatures of the strain variation (M_s, M_f) on cooling (a), (c), (e) and (A_s, A_f) heating (b), (d), (f) under stress of 200 MPa (a)–(d) or 300 MPa (e), (f). Temperatures were measured in T1 sample (a), (b) or T2 samples (c)–(f). Upper case shows the layer number where the transformation occurred.

heating was in the same temperature range as the reverse transformation in the 2nd layer (see table 1, figure 2(b)). Thus, the temperatures of this stage were denoted as A_s^2 and A_f^2.

On cooling and heating of T2 sample under stress, one stage of strain variation was observed both on cooling and heating (figures 3(b), (d)) within the temperature range of the forward and reverse transformation in the 3rd and 4th layers. As the M_s and A_f temperatures in the 3rd layer were larger than in the 4th layer, while the M_f and A_s temperatures in the 4th layer were lower than in the 3rd layer, then the strain variation on cooling started at the M_s^3 temperature and finished at the M_f^4 temperatures, whereas the strain recovery on heating started at the A_s^4 temperature and finished at A_f^3 temperatures. Temperature ranges of the transformation in the 3rd and 4th layers were overlapped that was why strain variation in these layers was observed in one stage.

The variation in the temperatures of the strain stages on thermal cycling under stress is given in figure 4. On thermal cycling under stress of 200 MPa, the M_s^2, M_f^2, A_s^2 and A_f^2 temperatures of the transformation in the 2nd layer decreased in the T1 sample (figures 4(a)–(b), while the M_s^3, M_f^4, A_s^4 and A_f^3 temperatures did not change both in the T1 sample (figures 4(a)–(b) and in the T2 sample (figures 4(c)–(d). On thermal cycling of T2 sample under 300 MPa, the A_f^3 temperature decreased, whereas the M_s^3, M_f^4 and A_s^4 temperatures were stable (figures 4(e)–(f). In the T1 sample, in the first cycle under 300 MPa, the transformation temperatures were $M_s^2 = 73$ °C, $M_f^2 = 57$ °C, $M_s^3 = 35$ °C, $M_f^4 = 0$ °C, $A_s^4 = 62$ °C, $A_f^3 = 83$ °C, $A_s^2 = 135$ °C and $A_f^2 = 150$ °C. On the second cooling, the temperatures were $M_s^2 = 80$ °C, $M_f^2 = 70$ °C, $M_s^3 = 42$ °C, $M_f^4 = 13$ °C. At the end of second cooling under 300 MPa, the T1 sample was broken. The comparison of the forward transformation temperatures during first and second cooling of T1 sample under 300 MPa showed that the temperatures increased that may be attributed to the influence of the plastic strain on the transformation [1]. As the T1 sample did not undergo more than one and half cycles under 300 MPa, it was excluded from further analysis.

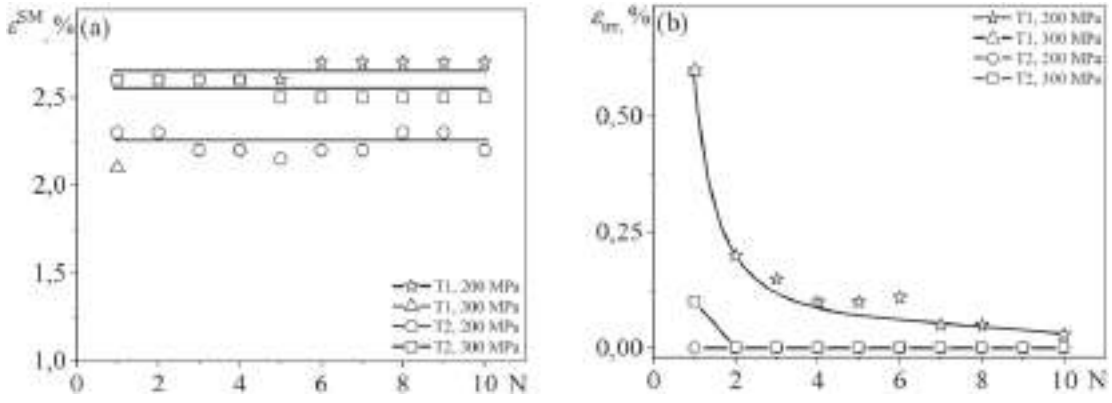

Figure 5. Dependences of recoverable strain (ε^{SM}) (a) and irreversible (ε_{irr}) (b) strain on the cycle number (N) obtained on cooling and heating under a stress in the NiTi alloy produced by WAAM.

Comparing the data found on cycling of T1 and T2 samples under 200 MPa and on cycling of T2 sample under 300 MPa, one may conclude that the temperatures of the transformation were stable in the Ni-rich NiTi layers of the WAAM sample (M_s^3, M_f^4, A_s^4 and A_f^3), while the temperatures of the same transformation in the Ti-rich NiTi layer (M_s^2, M_f^2, A_s^2 and A_f^2) were unstable. An increase in stress acting on cooling hardly affected the variation in the transformation temperatures tin he Ni-rich NiTi layers during thermal cycling.

Figure 5 showed the dependences of recoverable and irreversible strain on the thermocycle number. It is seen that the recoverable strain (ε^{SM}) was stable on thermal cycling of both T1 and T2 samples regardless of the stress acting on cooling and heating (figure 5(a)). Thus, it may be concluded that the strain variation was less sensitive to the structure of the NiTi alloy produced by WAAM contrary to the observation in the NiTi alloys produced by conventional way where the recoverable strain increased or decreased on thermal cycling depending on stress [25–29]. At the same time, the variation in irrecoverable strain depended on the stress acting on thermal cycling of the studied samples (figure 5(b)). In the T1 sample, the irrecoverable strain was 0.6% in the 1st cycle under 200 MPa and it decreased on further thermal cycling. In T2 sample, the plastic strain was zero during thermal cycling under 200 MPa and it was 0.1% in the 1st cycle under 300 MPa that decreased to zero in the 2nd and further cycles.

The results of paper showed that the NiTi sample produced by WAAM including the layers with the various chemical composition demonstrated different stability of functional behaviour on thermal cycling. In NiTi alloys produced by conventional technologies, the thermal cycling stability of the functional properties depended on the chemical composition, heat treatment, the presence/absence of precipitates, the initial density of defects (dislocations), the preliminary deformation [25, 28–31]. In the NiTi samples produced by WAAM, the preliminary deformation was equal zero, the heat-treatment and dislocation density were the same for all layers. At the same time, the chemical composition of the NiTi phase and the type of precipitates were different in the layers.

The various chemical compositions in the layers were due to the deposition of the first layer led to partial melting of the titanium substrate that increased the Ti concentration in the NiTi melt. As a result, the first layer was enriched by Ti elements that resulted in the formation of the Ti-rich NiTi phase and a lot of coarse Ti_2Ni particles. During the deposition of the second layer, the first layer was partially remelted and excess of Ti atoms came to the NiTi melt of the second layer. The concentration of Ti atoms were less than in the first layer however, it was enough to increase the Ti concentration from 49.2 at. % in wire used for deposition to 50.5 at. % in the second layer (measured in [10]). In the third layer the concentration of the Ti in the NiTi phase was 49.6 at %. Starting the fourth layer, the Ti content was close to nominal composition in the wire. The coarse Ti_2Ni particles were observed in the first and second layers, while fine precipitates of this phase were found on the grain boundaries in the third and next layers [10]. The heat treatment at 450 °C hardly affected the structure and chemical composition in the 1st—3rd layers due to the Ni concentration was 50.5 at. % or less (see [1]). In Ni-rich layers (the 4th and 5th), annealing decreased the Ni concentration by 50.5 at. % due to the formation of Ni_4Ti_3 precipitates in the grain interior [10]. Thus, after WAAM manufacturing and annealing, the five-layered wall had different chemical composition of the NiTi phase and various precipitates in layers that affected the martensitic transformation. T1 sample included the second layer with Ti-rich NiTi phase which underwent the B2 ↔ B19' martensitic transformation at high temperatures; the third layer with Ni-rich NiTi phase where the B2 → B19' occurred at low temperatures; and the 4th Ni-rich NiTi layer which anderwent the B2 →R → B19'

transformation at low temperatures (the intermediate R phase appeared due to the presence of the Ni_4Ti_3 precipitates). T2 sample included the third and fourth layers only.

The Ni-rich NiTi layers (3rd and 4th) were characterised by a high yield limit for dislocation slip due to two reasons. First of all, according to [32], the larger the Ni concentration in the NiTi phase, the higher the yield limit for dislocation slip. In the 4th layer, the Ni_4Ti_3 precipitates additionally increased the yield limit for dislocation slip [1]. A high yield limit for dislocation slip suppressed the plastic strain during thermal cycling in these layers, as a result, the temperatures of the transformation and recoverable strain did not change, while the irrecoverable strain was negligible. That is why the T2 sample including the Ni-rich NiTi layers only demonstrated the stable functional properties during thermal cycling.

The equiatomic or Ti-rich NiTi layer was characterized by a small yield limit for dislocation slip (see [32]), as a result, the plastic deformation occurred on thermal cycling under stress that changed the transformation temperatures and led to accumulation of the irreversible plastic strain. T1 sample included both the Ti-rich NiTi phase with unstable functional properties (the second layer) and the Ni-rich NiTi phase with the stable functional properties (the third and fourth layers) and this sample demonstrated unstable transformation temperatures. Thus, the existence of the second layer in the working length was the reason for the unstable functional properties observed during thermal cycling of the T1 sample. This is confirmed by the temperature variation on cycle number in T1 sample where it is seen that the temperatures of the first stage on the $\varepsilon(T)$ curve induced by the transformation in the second layer changed with cycles, whereas the temperatures of the second stage on the $\varepsilon(T)$ curve caused by the transformation in the 3rd and 4th layers were stable (figures 4(a), (b).

An increase in stress from 200 to 300 MPa increased the transformation temperatures according to Clausius–Clapeyron relation [1] but it hardly affected the variation in functional properties during thermal cycling. This was due to the recoverable strain variation in the NiTi samples produced by WAAM were first controlled by [001] texture which appeared during solidification [5, 7, 13, 15, 19, 20, 22]. According to [24], the [001] orientation single crystal demonstrated the smallest recoverable strain and increase in stress hardly affected this value. It is important to note that the plastic strain was the same in T1 sample after the first cycle under 200 or 300 MPa. However, this sample underwent 10 thermal cycles under 200 MPa without failure and it was broken on the second cooling under 300 MPa. This experiment was repeated for three samples and in all cases T1 sample was broken on the second cooling under 300 MPa. One may assume that the failure was caused by combine action of two reasons: large plastic strain and high stress.

4. Conclusions

Therefore, the results of the paper may be summarized as follows:

1. The NiTi sample produced by WAAM including the Ti-rich NiTi layer in the working length demonstrated unstable properties. The irreversible strain was observed on thermal cycling that affected the martensitic transformation temperatures in this layer during thermal cycling. This was typical for the conventional NiTi alloys with the same chemical composition where the defect density increased during thermal cycling due to a low dislocation yield limit.
2. The NiTi sample produced by WAAM including the Ni-rich NiTi layers only, demonstrated the stable recoverable strain and transformation temperatures during thermal cycling. The irreversible strain was the smallest and observed only in the first cycle under a high stress. Such behaviour was typical for the conventional Ni-rich NiTi alloys hardened by Ni_4Ti_3 precipitates.
3. The variation in the functional properties during thermocycling of the NiTi samples produced by WAAM, was controlled by the same factors (chemical composition of the NiTi phase and precipitate type) as in the NiTi alloys manufactured by conventional techniques. To avoid the variation in the functional behaviour on thermal cycling of the NiTi alloys produced by WAAM it is necessary to exclude the equiatomic or Ti-rich NiTi layers from the deformation.

Acknowledgments

This work was supported by joint DST-RSF project (RSF # 19-49-02014, DST #DST/INT/RUS/RSF/P-36).

Data availability statement

All data that support the findings of this study are included within the article (and any supplementary files).

ORCID iDs

Rashid Bikbaev https://orcid.org/0000-0002-7571-9058
Natalia Resnina https://orcid.org/0000-0002-0758-1325
Sergey Belyaev https://orcid.org/0000-0002-6184-3904

References

[1] Otsuka K and Ren X 2005 Physical metallurgy of Ti–Ni-based shape memory alloys *Prog. Mater Sci.* **50** 511–678
[2] Razov A I 2004 Application of titanium nickelide-based alloys in engineering *Phys. Met. Metallogr.* **97** 97–126
[3] Mohd Jani J, Leary M, Subic A and Gibson M A 2014 A review of shape memory alloy research, applications and opportunities *Mater. Des.* **56** 1078–113
[4] Elahinia M, Shayesteh Moghaddam N, Taheri Andani M, Amerinatanzi A, Bimber B A and Hamilton R F 2016 Fabrication of NiTi through additive manufacturing: a review *Prog. Mater Sci.* **83** 630–63
[5] Wang J, Pan Z, Yang G, Han J, Chen X and Li H 2019 Location dependence of microstructure, phase transformation temperature and mechanical properties on Ni-rich NiTi alloy fabricated by wire arc additive manufacturing *Mater. Sci. Eng.* A **749** 218–22
[6] Wang J, Pan Z, Wang Y, Wang L, Su L, Cuiuri D, Zhao Y and Li H 2020 Evolution of crystallographic orientation, precipitation, phase transformation and mechanical properties realized by enhancing deposition current for dual-wire arc additive manufactured Ni-rich NiTi alloy *Addit. Manuf.* **34** 101240
[7] Zeng Z, Cong B, Oliveira J P, Ke W, Schell N, Peng B, Qi Z W, Ge F, Zhang W and Ao S S 2020 Wire and arc additive manufacturing of a Ni-rich NiTi shape memory alloy: microstructure and mechanical properties *Addit. Manuf.* **32** 101051
[8] Pu Z, Du D, Wang K, Liu G, Zhang D, Wang X and Chang B 2021 Microstructure, phase transformation behavior and tensile superelasticity of NiTi shape memory alloys fabricated by the wire-based vacuum additive manufacturing *Mater. Sci. Eng.*A **812** 141077
[9] Resnina N, Palani I A, Belyaev S, Singh S, Mani Prabu S S, Bikbaev R, Jayachandran S and Kalganov V 2021 Peculiarities of the recoverable strain variation in the NiTi alloy produced by wire arc additive manufacturing *Mater. Lett.* **298** 130004
[10] Resnina N *et al* 2021 Structure, martensitic transformations and mechanical behaviour of NiTi shape memory alloy produced by wire arc additive manufacturing *J. Alloys Compd.* **851** 156851
[11] Ponikarova I *et al* 2021 The effect of substrate and arc voltage on the structure and functional behaviour of NiTi shape memory alloy produced by wire arc additive manufacturing *J. Manuf. Process.* **70** 132–9
[12] Resnina N *et al* 2021 Influence of heat treatment on the structure and martensitic transformation in NiTi alloy produced by wire arc additive manufacturing *Materialia* **20** 101238
[13] Wang J, Pan Z, Carpenter K, Han J, Wang Z and Li H 2021 Comparative study on crystallographic orientation, precipitation, phase transformation and mechanical response of Ni-rich NiTi alloy fabricated by WAAM at elevated substrate heating temperatures *Mater. Sci. Eng.* A **800** 140307
[14] Han J, Chen X, Zhang G, Lu L, Xin Y, Liu B, Cai Y, Zhang X and Tian Y 2022 Microstructure and mechanical properties of Ni50.8Ti49.2 and Ni53Ti47 alloys prepared *in situ* by wire-arc additive manufacturing *J. Mater. Process. Technol.* **306** 117631
[15] Resnina N, Palani I A, Belyaev S, Singh S, Kumar A, Bikbaev R and Sahu A 2022 Functional properties of the multilayer NiTi alloy produced by wire arc additive manufacturing *Shape Mem. Superelasticity* **8** 5–15
[16] Zhang M, Duan Y, Fang X, Zhang H, Jiao G, Li Y and Huang K 2022 Tailoring the superelasticity of NiTi alloy fabricated by directed energy deposition through the variation of residual stress *Mater. Des.* **224** 111311
[17] Yu L, Chen K, Zhang Y, Liu J, Yang L and Shi Y 2022 Microstructures and mechanical properties of NiTi shape memory alloys fabricated by wire arc additive manufacturing *J. Alloys Compd.* **892** 162193
[18] Resnina N, Palani I A, Belyaev S, Bikbaev R, Singh S, Mani Prabu S S and Jayachandran S 2022 Influence of annealing on the functional properties of the NiTi alloy produced by wire arc additive manufacturing *IOP Conf. Ser.: Mater. Sci. Eng.* **1213** 012002
[19] Teng J Z, Jiang P F, Cui X H, Nie M H, Li X R, Liu C Z and Zhang Z H 2023 Revealing microstructural evolutions, mechanical properties and wear performance of wire arc additive manufacturing homogeneous and heterogeneous NiTi alloy *J. Mater. Res. Technol.* **27** 1593–610
[20] Resnina N, Palani I A, Belyaev S, Bikbaev R, Ponikarova I, Geethapriyan T and Starodubova M 2023 Influence of Substrate Temperature on Structure and Functional Properties of NiTi Walls Produced by WAAM *Trans. Indian Inst. Met* **77** 987–995
[21] Kumar A, Palani I A and Yadav M 2024 Comprehensive study of microstructure, phase transformations, and mechanical properties of nitinol alloys made of shape memory and superelastic wires and a novel approach to manufacture Belleville spring using wire arc additive manufacturing *Mater. Today Commun.* **38** 107881
[22] Ke W cc, Oliveira J P P, Cong B Q Q, Ao S S S, Qi Z W W, Peng B and Zeng Z 2022 Multi-layer deposition mechanism in ultra high-frequency pulsed wire arc additive manufacturing (WAAM) of NiTi shape memory alloys *Addit. Manuf.* **50** 102513
[23] Zhang M, Li X, Wang B, Jiao G, Yang Y, Fang X and Huang K 2024 Prominent superelastic response induced by Ni4Ti3 phase in NiTi alloys fabricated via wire-arc directed energy deposition *Mater. Sci. Eng.* A **897** 146366
[24] Gall K, Sehitoglu H, Chumlyakov Y I and Kireeva I V 1999 Tension–compression asymmetry of the stress–strain response in aged single crystal and polycrystalline NiTi *Acta Mater.* **47** 1203–17
[25] Miyazaki S, Igo Y and Otsuka K 1986 Effect of thermal cycling on the transformation temperatures of TiNi alloys *Acta Met.* **34** 2045–51
[26] Furuya Y and Park Y C 1992 Thermal cyclic deformation and degradation of shape memory effect in Ti-Ni alloy *Nondestr. Test. Eval* **8–9** 541–54
[27] Wagner M F-X F X, Dey S R R, Gugel H, Frenzel J, Somsen C and Eggeler G 2010 Effect of low-temperature precipitation on the transformation characteristics of Ni-rich NiTi shape memory alloys during thermal cycling *Intermetallics* **18** 1172–9
[28] Pelton A R R, Huang G H H, Moine P and Sinclair R 2012 Effects of thermal cycling on microstructure and properties in nitinol *Mater. Sci. Eng.* A **532** 130–8
[29] Tadaki T, Nakata Y and Shimizu K 1987 Thermal cycling effects in an aged Ni-rich Ti-Ni shape memory alloy *Trans. Japan Inst. Met.* **28** 883–90
[30] Frick C P, Ortega A M, Tyber J, Maksound A E M, Maier H J, Liu Y and Gall K 2005 Thermal processing of polycrystalline NiTi shape memory alloys *Mater. Sci. Eng.* A **405** 34–49
[31] Tang W and Sandström R 1993 Analysis of the influence of cycling on TiNi shape memory alloy properties *Mater. Des.* **14** 103–13
[32] Melton K N and Mercier O 1981 The mechanical properties of NiTi-based shape memory alloys *Acta Metall.* **29** 393–8